DMD Fast Forward. Published on December 3, 2007 as doi:10.1124/dmd.107.018556
This article has not been copyedited and formatted. The final version may differ from this version.

P-glycoprotein restricts the penetration of oseltamivir across the blood-brain barrier.

Atsushi Ose, Hiroyuki Kusuhara PhD., Kenzo Yamatsugu, Motomu Kanai PhD., Masakatsu Shibasaki PhD., Takuya Fujita PhD., Akira Yamamoto PhD., Yuichi Sugiyama PhD.

The Graduate School of Pharmaceutical Sciences, the University of Tokyo, Bunkyo-ku, Tokyo, Japan (A.O., H.K., K.Y., M.K., M.S., Y.S.)

Ritsumeikan University, Kusatsu, Shiga, Japan (T.F.)

Kyoto Pharmaceutical University, Yamashina-ku, Kyoto, Japan (A.Y.)

DMD Fast Forward. Published on November 26, 2007 as DOI: 10.1124/dmd.107.018556
This article has not been copyedited and formatted. The final version may differ from this version.

Running title : Active efflux of oseltamivir by P-gp at the BBB

Corresponding author : Yuichi Sugiyama

Address: Department of Molecular Pharmacokinetics, Graduate School of Pharmaceutical Sciences, The University of Tokyo, 7-3-1 Hongo, Bunkyo-ku, Tokyo 113-0033, Japan

Phone : +81-3-5841-4770

Fax : +81-3-5841-4767

E-mail : sugiyama@mol.f.u-tokyo.ac.jp

Number of Text Pages: 26

Figures: 8

Tables: 1

References: 36

Number of Words: Abstract: 250

Introduction: 645

Discussion: 1230

Abbreviations :

BBB, blood-brain barrier; P-gp, P-glycoprotein; Bcrp, breast cancer resistance protein; OAT, organic anion transporter; CES, carboxylesterase; $K_{p,brain}$, brain-to-plasma concentration ratio; BSA, bovine serum albumin

DMD Fast Forward. Published on November 26, 2007 as DOI: 10.1124/dmd.107.018556
This article has not been copyedited and formatted. The final version may differ from this version.

Abstract

Oseltamivir is an ethyl ester prodrug of Ro 64-0802, the anti-influenza drug. Abnormal behavior has been suspected to be associated with oseltamivir medication in Japan. The purpose of the present study is to examine the involvement of transporters in the brain distribution of oseltamivir and its active form Ro 64-0802 across the blood-brain barrier. The brain-to-plasma concentration ratio ($K_{p,brain}$) of oseltamivir after intravenous infusion of oseltamivir in FVB mice was increased by pretreatment with GF120918, a dual inhibitor for P-glycoprotein (P-gp) and breast cancer resistance protein (Bcrp), while that of Ro 64-0802 was only slightly increased. Furthermore, the distribution volume of Ro 64-0802 following intravenous administration of Ro 64-0802 in the brain was similar to the capillary volume, suggesting its minimal distribution. The $K_{p,brain}$ value of oseltamivir in Mdr1a/1b P-gp knockout mice was 5.5-fold higher than that in wild-type mice, and comparable with that obtained by pretreatment with GF120918, while it was unchanged in Bcrp knockout mice. The $K_{p,brain}$ value of oseltamivir was significantly higher in newborn rats, which is in good agreement with the ontogenetic expression profile of P-gp. Intracellular accumulation of oseltamivir was lower in human and mouse P-gp-expressing cells, which was reversed by P-gp inhibitor PSC833. These results suggest that P-gp limits the brain uptake of oseltamivir at the blood-brain barrier, and that Ro 64-0802 itself barely crosses the blood-brain barrier. However, it may be possible that Ro 64-0802 is formed in the brain from the oseltamivir, considering the presence of CES in the brain endothelial cells.

DMD Fast Forward. Published on November 26, 2007 as DOI: 10.1124/dmd.107.018556
This article has not been copyedited and formatted. The final version may differ from this version.

Introduction

Oseltamivir (Fig. 1) is an ester prodrug of Ro 64-0802, a potent and selective inhibitor of neuraminidase, resulting in an inhibition of release of influenza virus from the host cells and growth of influenza virus. Oseltamivir is used in the treatment and prophylaxis of both Influenzavirus A and Influenzavirus B (Bardsley-Elliot and Noble, 1999). The number of prescribed oseltamivir has reached approximately 10 million in Japan, which accounted for 75 percent of the world total in 2006. Recently, abnormal behavior has been reported in influenza patients prescribed oseltamivir (http://www.fda.gov/cder/drug/infopage/tamiflu/QA20051117.htm; Fuyuno, 2007) According to a report by the Ministry of Health, Labor and Welfare, the number of people who behaved abnormally following oseltamivir treatment has risen to 211 (0.002% of all patients), approximately 80 percent of whom are teenagers or younger. The relationship between abnormal behavior and oseltamivir medication remains an open question, and has not yet been elucidated. The Ministry of Health, Labor and Welfare has published a caution for oseltamivir medication to teenagers or younger people. Recently, it was demonstrated that oseltamivir and Ro 64-0802 affects neuronal excitability in rat hippocampal slices, and Ro 64-0802 exhibits 30 times more potent than oseltamivir (Izumi et al., 2007). Based on these backgrounds, there is growing interest in the penetration of oseltamivir and its active form Ro 64-0802 into the brain.

The purpose of the present study was to characterize the transport of oseltamivir and Ro 64-0802 across the blood-brain barrier (BBB). Oseltamivir is rapidly hydrolyzed to its active form, Ro 64-0802, by human carboxylesterase 1 (hCES1) in the liver (Shi et al., 2006), and then exclusively excreted into the urine by glomerular filtration and active tubular secretion via organic anion transporter 1 (OAT1) without further metabolism (He et al., 1999). In healthy volunteers, both oseltamivir and Ro 64-0802 were detected in the blood circulation although the C_{max} of oseltamivir was 6-fold smaller than that of Ro 64-0802 (He et al., 1999). The penetration of drugs into the brain is limited by the BBB formed by the brain capillary endothelial cells. Because of highly developed tight junctions between adjacent cells, and a paucity of fenestra and pinocytotic vesicles, the penetration across the paracellular route is very limited, and thus, transcellular transport across

the endothelial cells is the major pathway. Therefore, there is a good correlation between BBB permeability and lipophilicity. As oseltamivir is an ester-type prodrug, it should exhibit higher BBB permeability than Ro 64-0802. hCES1 is also expressed in the brain at mRNA level (Satoh et al., 2002), and may convert oseltamivir to Ro 64-0802 in the brain, leading to an accumulation of Ro 64-0802 in the brain once oseltamivir penetrates the brain across the BBB in addition to the direct penetration of Ro 64-0802 from the systemic circulation. In addition to the physiological characteristics of the BBB, it has been accepted that active efflux across the BBB also provides a barrier function to the BBB. P-glycoprotein (P-gp), a 170 kDa membrane protein, is a well-known gatekeeper protein in the BBB that plays a pivotal role in limiting the brain penetration of a range of xenobiotic compounds (Schinkel et al., 1994; Tamai and Tsuji, 2000; Kusuhara and Sugiyama, 2001). In addition to P-gp, recently it was found that breast cancer resistance protein (BCRP/ABCG2) also acts as active efflux pump in the BBB, and functional impairment of Bcrp results in an significant increase in the brain concentrations of imatinib (Breedveld et al., 2005) and phytoestrogens (Enokizono et al., 2007). These transporters may limit the exposure of the brain to oseltamivir and/or Ro 64-0802.

In the present study, the effect of GF120918 on the brain distribution of oseltamivir and Ro 64-0802 was examined in wild-type mice to suggest transporters involved in the efflux transport across the BBB. To support this in vivo inhibition study, the brain-to-plasma concentration ratios were determined in both Mdr1a/1b P-gp and Bcrp knockout mice.

Materials and Methods

Reagents and Animals.

Oseltamivir phosphate and its active metabolite Ro 64-0802 were synthesized (Yamatsugu et al., 2007). GF120918 (Elacridar) was a gift from GlaxoSmithKline (Ware, UK). PSC 833 was kindly supplied by Novartis Pharma AG (Basel, Switzerland). Mouse Mdr1a-expressed LLC-PK1 cells (Schinkel et al., 1995) were a gift from Dr. Alfred H. Schinkel (The Netherlands Cancer Institute, Amsterdam, The Netherlands), and human MDR1-expressed MDCKII cells (Evers et al., 2000) were kindly provided by Dr. Piet Borst (The Netherlands Cancer Institute, Amsterdam, The Netherlands). All other chemicals used in the experiments were of analytical grade.

Male FVB mice, Mdr1a/1b P-gp knockout mice, and Bcrp knockout mice were obtained from Taconic (USA), and maintained in Shimizu Laboratory Supplies (Kyoto, Japan). Male Wistar rats were supplied by Charles River (Kanagawa, Japan). All mice (10-18 weeks) and rats (3-42 days) were maintained under standard conditions with a reverse dark-light cycle. Food and water were available ad libitum. All experiments using animals in this study were carried out according to the guidelines provided by the Institutional Animal Care Committee (Graduate School of Pharmaceutical Sciences, The University of Tokyo).

In Vivo Infusion Study in Mice and Rats.

Male FVB mice, Mdr1a/1b P-gp knockout mice, and Bcrp knockout mice (10-18 weeks) weighing approximately 25 to 35 g and male Wistar rats (3-42 days) weighing approximately 10 and 200 g, respectively, were used for these experiments. Under pentobarbital anesthesia (30 mg/kg), the jugular vein was cannulated with a polyethylene-10 catheter for the injection of oseltamivir and Ro 64-0802. GF120918 (10 mg/3.3 mL/kg, dissolved in a 3:2 mixture of propylene glycol/water) was injected intravenously to male FVB mice 15 min before the intravenous infusion of oseltamivir and Ro 64-0802. The mice and rats then received a constant intravenous infusion of oseltamivir and Ro 64-0802 at a dose of 8 μmol/hr/kg and 5 μmol/hr/kg, respectively. Blood samples were collected from the jugular vein at 60, 90, and 120 min in mice and 20, 40, and 60 min in rats.

DMD Fast Forward. Published on November 26, 2007 as DOI: 10.1124/dmd.107.018556
This article has not been copyedited and formatted. The final version may differ from this version.

Plasma was prepared by centrifugation of the blood samples (10,000*g*). Esterase inhibitor, dichlorvos (200 μg/mL), was used to prevent ex vivo hydrolysis of oseltamivir to Ro 64-0802 in the blood and plasma (Wiltshire et al., 2000; Lindegardh et al., 2006). The mice and rats were sacrificed after 120 and 60 min, respectively, and the brain was excised immediately. The tissues were weighed and stored at -80 °C until used.

Quantification of Mdr1a mRNA expression in Rat Cerebral Cortex.

The mRNA levels of Mdr1a and gapdh were quantified by the real-time polymerase chain reaction (PCR) method. Total RNA was isolated from rat cerebral cortex pooled from 1-4 rats using ISOGEN (Wako Pure Chemicals). Real-time PCR was performed with a QuantiTect SYBR Green PCR Kit (QIAGEN, Valencia, CA) and a LightCycler system (Roche Diagnostics, Mannheim, Germany). The following primers were designed: Mdr1a forward AACTTAGTCTATGGG GGAGG, reverse ACCACACCTTTCTGCTTACA; gapdh forward AGCCCAGAACATCATCCCTG, reverse CACCACCTTCTTGATGTCATC. An external standard curve was generated by dilution of the target PCR product, which was purified by agarose gel electrophoresis. The absolute concentration of the external standard was measured with PicoGreen dsDNA Quantification Reagent (Molecular Probes, Eugene, OR).

Western Blot Analysis.

Crude membranes from rat cerebral cortex were prepared as follows. After the addition of cold PBS at a ratio of 1 g cerebral cortex/4 mL, the cerebral cortex pooled from 1-4 rats were homogenized using a Polytron homogenizer. The homogenate was centrifuged at 4 °C for 15 min at 2000g, and the supernatant was collected and centrifuged at 4 °C for 15 min at 100,000g. The resultant pellet was resuspended in PBS containing 0.1% protease inhibitor cocktail (Sigma-Aldrich) and stored at -80 °C until used. The protein concentration was measured by the Lowry method. The specimens were loaded onto an 8.5% SDS-PAGE with a 3.75% stacking gel. Proteins were electroblotted onto a polyvinylidene difluoride membrane (Pall, Port Washington, NY). The

membrane was blocked with Tris-bufer saline containing 0.05% Tween 20 (TTBS) and 2.5% ECL Advance Blocking Agent (Amersham Biosciences) for 1 hr at room temperature. After washing with TTBS, the membrane was incubated with monoclonal anti-P-gp C219 antibody (Signet Laboratories; 1:100 in TTBS containing 2.5% ECL Advance Blocking Agent) overnight at 4 °C. Detection was carried out by binding a horseradish peroxidase-labeled anti-mouse IgG antibody (Amersham Bioscience; 1:5000 in TTBS containing 2.5% ECL Advance Blocking Agent). Immunoreactivity was detected with an ECL Advance Western Blotting Detection Kit (Amersham Biosciences). The intensity of the band was quantified by Multi Gauge software Ver 2.0 (Fujifilm, Tokyo, Japan). Stripping of membranes was performed with Restore Western Blot Stripping buffer (Pierce) for 30 min at 37 °C. After washing with TTBS, the membrane was blocked with TTBS containing 5% skim milk for 1 hr at room temperature. After washing with TTBS, the membrane was incubated with monoclonal anti-actin antibody (Chemicon; 1:1000 in TTBS containing 0.1% BSA) for 1 hr at room temperature. Detection was carried out by binding a horseradish peroxidase-labeled anti-mouse IgG antibody (Amersham Bioscience; 1:5000 in TTBS containing 0.1% BSA).

Rat Liver S9 Fraction Preparation.

Male Wistar rats (11 and 42 days) were anesthetized with ether, and their livers were quickly removed and washed in cold phosphate-buffered saline (PBS). The livers were blotted dry and weighed. After the addition of cold PBS at a ratio of 1 g liver/2 mL, the livers were homogenized using a glass homogenizer with a Teflon pestle. The homogenized liver was then centrifuged at 4 °C for 30 min at 9000g. Aliquots of the resulting supernatant were placed in several polypropylene tubes and stored at -80 °C until used. The protein concentration was measured by the Lowry method.

Ro 64-0802 Formation in Rat Plasma and Liver S9 Specimens.

A 0.5 ml incubation mixture contained 2.5 mg protein of rat plasma or liver S9 in PBS. After temperature equilibration (37 °C, 5 min), the incubation was started by adding 5 µl of

oseltamivir (final 1.5 μM) and performed for various time periods up to 30 and 180 min for plasma and liver S9, respectively. After the reaction was terminated by ethanol, the concentrations of oseltamivir and Ro 64-0802 were determined with liquid chromatography/mass spectrometry (LC/MS) analysis.

Ro 64-0802 formation rates in the plasma protein or liver S9 protein were extrapolated to the in vivo value by taking the plasma protein content (50 mg plasma protein/mL) or liver S9 protein content (96.1 mg S9 protein/g liver (Izumi et al., 1997)) per milliliter plasma or gram liver, respectively, into consideration. Furthermore, Ro 64-0802 formation rates expressed per milliliter plasma or gram liver were expressed per kilogram body weight by taking the plasma content (38.5 mL plasma/kg weight) or liver weight (40 g liver/kg weight) per kilogram body weight into consideration.

Cellular Accumulation Studies.

Mouse Mdr1a-expressed LLC-PK1 cells and human MDR1-expressed MDCKII cells were maintained as described with minor modifications. Uptake was initiated by adding the compounds to the incubating buffer in either the presence or the absence of 5 μM PSC833 after cells had been washed twice and preincubated with Krebs-Henseleit buffer at 37 °C for 15 min. The Krebs-Henseleit buffer consisted of 142 mM NaCl, 23.8 mM $NaHCO_3$, 4.83 mM KCl, 0.96 mM KH_2PO_4, 1.20 mM $MgSO_4$, 12.5 mM HEPES, 5 mM glucose, and 1.53 mM $CaCl_2$ adjusted to pH 7.4. The uptake was terminated at designated times by adding ice-cold Krebs-Henseleit buffer, and the cells were washed twice. After the cells were suspended in water, the concentration of the compounds was determined with LC/MS analysis. The protein concentration was measured using the Lowry method. Cellular uptake is given as the cell-to-medium concentration ratio determined as the amount of compound associated with cells divided by the medium concentration.

Quantification of Oseltamivir and Ro 64-0802 in Plasma and Brain.

Sample Preparation. The brain was homogenized with a fourfold volume of PBS to obtain a 20%

brain homogenate. The plasma samples (10 µl) were mixed with 40 µl of ethanol; and the brain homogenates (100 µl) were mixed with 400 µl of ethanol. All these mixed solutions were centrifuged at 15,000g for 10 min. The supernatants of brain sample (350 µl) were evaporated, and the pellets were reconstituted with 50 µl of 20% ethanol. The reconstituted samples were centrifuged at 15,000g for 10 min to remove particles and an aliquot of the supernatant was subjected to LC/MS analysis. The supernatants of plasma sample were mixed with an equal volume of water and subjected to LC-MS analysis.

LC/MS Analysis. An LC/MS-2010 EV equipped with a Prominence LC system (Shimadzu, Kyoto, Japan) was used for the analysis. Samples were separated on a CAPCELL PAK C18 MGII column (3 µm, 2 mm x 50 mm; Shiseido, Tokyo, Japan) in binary gradient mode with flow rate at 1 mL/min. For the mobile phase, 0.05% formic acid and acetonitrile were used. The acetonitrile concentration was initially 10%, and then linearly increased up to 40% over 2 min. Finally, the column was reequilibrated at an acetonitrile concentration of 10% for 3 min. The total run time was 5 min. Oseltamivir and Ro 64-0802 were eluted at 2.5 and 3.5 min, respectively. In the mass analysis, oseltamivir and Ro 64-0802 were detected at a mass-to-charge ratio of 313.20 and 285.15 under positive electron spray ionization conditions, respectively. The interface voltage was –3.5 kV, and the nebulizer gas (N_2) flow was 1.5 L/min. The heat block and curved desolvation line temperatures were 200 °C and 150 °C, respectively.

Pharamacokinetic Analysis.

The apparent brain-to-plasma concentration ratio ($K_{p,brain}$) was calculated using the following equation:

$$K_{p,brain}=C_{brain}/C_p$$

where C_{brain} and C_p represent brain concentration at 120 min in mice and 60 min in rats (nmol/g brain) and plasma concentration at 120 min in mice and 60 min in rats (µM), respectively.

DMD Fast Forward. Published on November 26, 2007 as DOI: 10.1124/dmd.107.018556
This article has not been copyedited and formatted. The final version may differ from this version.

Statistical Analysis.

Data are presented as the mean ± standard error (SE) for 3–7 animals unless specified otherwise. Student's two-tailed unpaired t test and one-way ANOVA followed by Tukey's multiple comparison test or Dunnett's Multiple Comparison Test were used to identify significant differences between groups when appropriate. Statistical significance was set at $P < 0.05$.

Results

Effect of Pretreatment with GF120918 on the Brain Distribution of Oseltamivir and Ro 64-0802.

FVB mice were pretreated with GF120918 (10 mg/kg, i.v. administration), a dual inhibitor for P-gp and Bcrp (Allen et al., 1999), 15 min before intravenous infusion of oseltamivir. The plasma concentrations of oseltamivir and Ro 64-0802 were increased by GF120918 (Fig. 2A). Furthermore, the brain-to-plasma concentration ratio ($K_{p,brain}$) of oseltamivir was 4.8-fold increased in the GF120918-treated group in comparison with the control group (Fig. 2B). The $K_{p,brain}$ of Ro 64-0802 was slightly increased by GF120918 (0.007 ± 0.001 versus 0.011 ± 0.002 mL/g brain) (Fig. 2B) without any statistical significance. The $K_{p,brain}$ of Ro 64-0802 after dosing with Ro 64-0802 was also found to be unchanged between GF120918-treated and control groups.

Effect of P-gp and Bcrp on the Brain Distribution of Oseltamivir and Ro 64-0802.

The plasma concentrations and $K_{p,brain}$ of oseltamivir and Ro 64-0802 were determined after dosing with oseltamivir in Mdr1a/1b P-gp knockout mice and Bcrp knockout mice. The plasma concentrations of oseltamivir were unchanged between wild-type and Mdr1a/1b P-gp knockout mice, while the $K_{p,brain}$ of oseltamivir was 5.5-fold greater in Mdr1a/1b P-gp knockout mice than that in wild-type mice (Fig. 3). The $K_{p,brain}$ of oseltamivir was unchanged in Bcrp knockout mice (Fig. 3B). The $K_{p,brain}$ of Ro 64-0802 following oseltamivir administration in Mdr1a/1b P-gp knockout mice and Bcrp knockout mice was not significantly different from that in wild-type mice (Fig. 3B).

The Brain Distribution of Oseltamivir in Newborn Rats and Adult Rats.

The plasma concentrations, brain concentrations, and $K_{p,brain}$ of oseltamivir were determined after dosing with oseltamivir in newborn and adult rats on postnatal day (P) 3, 6, 11, 21 and 42, respectively. The plasma and brain concentrations of oseltamivir in newborn rats were significantly higher than those in adult rats (Fig. 4). Ro 64-0802 was found to be below the limit of quantification in the brain of the newborn rats.

DMD Fast Forward. Published on November 26, 2007 as DOI: 10.1124/dmd.107.018556
This article has not been copyedited and formatted. The final version may differ from this version.

The mRNA and Protein Expression of Mdr1a in the Cerebral Cortex from Newborn Rats and Adult Rats.

The mRNA expression levels of Mdr1a in the cerebral cortex from P3-42 rats were determined using real-time quantitative PCR. The mRNA levels in the cerebral cortex from newborn rats (P3-11) were significantly lower as compared with those from adult rats (P42) (Fig. 5). The protein expression of P-gp in the crude membrane fraction of rat cerebral cortex from P3-42 was also examined by Westerb blot analysis. Two bands were observed around 175 kD by anti-P-gp monoclonal antibody (Fig. 6). Because the lower signal is likely (but not demonstrated) to be non-glycosylated P-gp (Maines et al., 2005), the densitometric analysis was performed for the upper signals as specific signals of matured P-gp. It was demonstrated that the expression levels of P-gp protein in the cerebral cortex form newborn rats were significantly lower than those from adult rats (Fig. 6).

Formation Rate of Ro 64-0802 from the Oseltamivir in the Plasma and Liver S9 from Newborn rats and Adult rats.

The enzymatic activities of hydrolytic reaction of oseltamivir to Ro 64-0802 were compared in newborn and adult rats using plasma and liver S9 specimens. Oseltamivir was more stable in both plasma and liver S9 from newborn rats than in those from adult rats (Fig. 7). The formation rates of Ro 64-0802 from oseltamivir in the plasma and liver S9 specimens are shown in Table 1. The formation rates of Ro 64-0802 in the plasma and liver S9 specimens of newborn rats were 16 and 35% of the adult rats, respectively (Table 1). Taking the scaling factors into consideration, the formation rate of Ro 64-0802 in plasma expressed per kilogram body weight was approximately 10- and 20-fold higher than that in liver S9 in both newborn and adult rats (Table 1).

DMD Fast Forward. Published on November 26, 2007 as DOI: 10.1124/dmd.107.018556
This article has not been copyedited and formatted. The final version may differ from this version.

Cellular Accumulation of Oseltamivir in mouse Mdr1a-expressed LLC-PK1 Cells and Human MDR1-expressed MDCKII Cells

To determine whether oseltamivir is a possible substrate for human and mouse P-gp, cellular accumulation studies were conducted using mouse Mdr1a-expressed LLC-PK1 cells (mMdr1a-LLC-PK1) and human MDR1-expressed MDCKII cells (hMDR1-MDCKII). Oseltamivir exhibited less accumulation in mMdr1a-LLC-PK1 and hMDR1-MDCKII than in each parent cell and PSC833 increased oseltamivir accumulation in both mMdr1a-LLC-PK1 and hMDR1-MDCKII (Fig. 8).

Discussion

In the present study, we investigated the transport of oseltamivir and Ro 64-0802 across the BBB using Mdr1a/1b and Bcrp knockout mice, and demonstrated that P-gp extrudes oseltamivir into the circulating blood.

The plasma and brain concentrations of oseltamivir were determined in wild-type mice following intravenous infusion of oseltamivir. The distribution volume of oseltamivir in the brain was greater than the capillary volume (Takasato et al., 1984; Rousselle et al., 1998), indicating that oseltamivir crosses the BBB. Pretreatment with GF120918, a dual inhibitor for P-gp and Bcrp (Allen et al., 1999), caused a significant increase in the brain concentration of oseltamivir. This is partly due to greater plasma concentrations of oseltamivir in GF120918-treated group, presumably because of an inhibition of esterase activity by GF120918 as oseltamivir is predominantly converted to Ro 64-0802 in mice, and the biliary and urinary excretion account for a limited part of the systemic elimination, at most 0.3 and 19%, respectively (data not shown). However, a significant increase in the $K_{p,brain}$ of oseltamivir by GF120918 indicates that inhibition of active efflux mediated by P-gp and/or Bcrp is another underlying mechanism (Fig. 2B). Unlike oseltamivir, the distribution volume of Ro 64-0802 was close to the capillary volume, and $K_{p,brain}$ of Ro 64-0802 following oseltamivir or Ro 64-0802 administration was slightly increased by the administration of GF120918, but the difference was not statistically significant. This would be reasonable considering the low lipophilicity of Ro 64-0802 that will exhibit low BBB permeability without the aid of uptake transporters.

To support the effect of GF120918, in vivo studies using Mdr1a/1b and Bcrp knockout mice were performed. The $K_{p,brain}$ of oseltamivir was significantly increased in Mdr1a/1b P-gp knockout mice, but not in Bcrp knockout mice (Fig. 3B). The increase in the $K_{p,brain}$ of Mdr1a/1b P-gp knockout mice was comparable to that obtained by GF120918 (Fig. 2B and 3B). Therefore, P-gp, but not Bcrp, limits the brain penetration of oseltamivir across the BBB. In accordance with the in vivo results, cellular accumulation study elucidated that both mouse Mdr1a P-gp and human P-gp accept oseltamivir as substrate since the cellular accumulation of oseltamivir was lower in a cell line

DMD Fast Forward. Published on November 26, 2007 as DOI: 10.1124/dmd.107.018556
This article has not been copyedited and formatted. The final version may differ from this version.

expressing mouse P-gp and human P-gp, which was increased by PSC833 treatment (Fig. 8).

The present study elucidated that the activity of P-gp is an important factor for the brain concentration of oseltamivir in mice. As abnormal behavior following oseltamivir medication is more frequently observed in younger generations than in adults, postnatal ontogeny of P-gp is an important issue. Mdr1a mRNA and P-gp protein levels were significantly lower in newborn rats than adult rats (Fig. 5 and 6). This result is in good agreement with previous reports, in which it has been demonstrated that adults had higher brain expression of Mdr1a mRNA (threefold), and a corresponding fivefold increase in immunodetectable P-gp (Matsuoka et al., 1999) (Goralski et al., 2006). Consistent with this ontogenic profile, the brain accumulation of cyclosporin A was 80% lower in adult mice than in one-day-old mice (Goralski et al., 2006). NDA documents reported that the $K_{p,brain}$ of oseltamivir, obtained by comparison of the area under the curve of the plasma and brain concentration time profiles, was dramatically greater in newborn rats than that in adult rats at very high doses of oseltamivir (1000 mg/kg, PO). The brain concentrations of oseltamivir in newborn rats were significantly higher than those in adult rats (Fig. 4B). This is partly due to greater plasma concentrations of oseltamivir in newborn rats than in adult rats (Fig. 4A); however, a significant increase in the $K_{p,brain}$ of oseltamivir in newborn rats suggests that the smaller efflux clearance across the BBB is part of the underlying mechanism. This is in good agreement with the postnatal ontogenic profile of P-gp (Matsuoka et al., 1999; Goralski et al., 2006).

Newborn rats exhibited greater plasma concentrations of oseltamivir, suggesting a smaller systemic elimination rate in newborn rats. This was confirmed by comparing the conversion activities (CES activity) in the plasma and liver S9 specimens between newborn (P11) and adult (P42) rats. In comparison with adult rats, the conversion activities (CES activity) were lower in both the plasma and the liver S9 specimens from newborn rats (Fig. 7 and Table 1). Lower conversion activity of oseltamivir to Ro 64-0802, particularly in the plasma, will account for the delay in the systemic elimination of oseltamivir in newborn rats.

Recent clinical studies support that P-gp acts as a gatekeeper protein in human BBB (Sadeque et al., 2000; Sasongko et al., 2005). P-gp will also be one of the determinant factors for the brain

concentrations of oseltamivir. Single nucleotide polymorphisms (SNPs) are the genetic factor for interindividual differences in drug response. A number of SNPs have been described in the human MDR1 gene (Fromm, 2002; Kim, 2002). Of these, linkage disequilibrium has been demonstrated between SNPs in exons 26 (C3435T), 21 (G2677T), and 12 (C1236T), and the TTT haplotype correlates with low P-gp activity in the small intestine (Chowbay et al., 2003). As far as the BBB is concerned, there was no significant relationship between the haplotype and brain concentrations of [^{11}C]verapamil (Brunner et al., 2005; Takano et al., 2006). However, Kimchi-Sarfaty et al. recently reported that the effect of double or triple haplotypes containing C3435T on P-gp activity is "substrate dependent" (Kimchi-Sarfaty et al., 2007). The possibility that SNPs of P-gp are associated with an interindividual difference in the BBB permeability of oseltamivir cannot be excluded. In addition to P-gp, as observed in newborn rats, the activity of hCES1 is the determinant factor for the systemic elimination. C70F and R128H of hCES1 were reported to be associated with reduced hydrolysis of oseltamivir (Shi et al., 2006). Subjects with these SNPs of hCES1 will result in a greater exposure of oseltamivir to the brain.

Ro 64-0802 is a potent and selective inhibitor of influenza virus neuraminidase (sialidase). Several sialidases are expressed in the human brain, and are suggested to be involved in the mitochondrial apoptotic pathway in neuronal cell death (Yamaguchi et al., 2005; Hasegawa et al., 2007). Inhibition of sialidases in the brain might be associated with the abnormal behavior following oseltamivir medication. Based on this speculation, production of Ro 64-0802 in the human brain will be the key event that triggers the CNS side effects. Unlike the ester-type prodrug, Ro 64-0802 barely penetrate into the brain from the circulating blood due to its hydrophilic property. As hCES1 is also expressed in the brain (Satoh et al., 2002), it is possible that Ro 64-0802 is formed in the brain from the oseltamivir. Because of low membrane permeability, Ro 64-0802, once produced in the brain from oseltamivir, may accumulate in the brain. It is also possible that Ro 64-0802 undergoes active efflux from the brain at the BBB because Ro 64-0802 is a substrate of renal organic anion transporter 1 (OAT1/*SLC22A6*) (Hill et al., 2002) and OAT3, the homologue of OAT1, is expressed at the BBB, and actively eliminates organic anions from the brain (Kikuchi et al., 2003;

Kikuchi et al., 2004). This should be examined in future.

In conclusion, the present study demonstrated that oseltamivir crosses the BBB, but the active form Ro 64-0802 barely crosses the BBB. P-gp limits the brain penetration of oseltamivir at the BBB of adult mice. Ontogenetic profile of P-gp and CES activities accounts for the greater accumulation of oseltamivir in the brain of neonates at least in rats.

Acknowledgments :

The authors thank Dr. Glynis Nicholls, GlaxoSmithKline Research & Development for the kind gift of GF120918, and Novartis Pharma AG for the kind gift of PSC833. We also thank Dr. Piet Borst (The Netherlands Cancer Institute) for providing the human MDR1-expressed MDCKII cells, Dr. Alfred H. Schinkel for providing the mouse Mdr1a-expressed LLC-PK1 cells, and Dr. Junko Iida and Futoshi Kurotobi (Shimadzu Corporation, Kyoto, Japan) for the technical support of LC/MS system.

References

Allen JD, Brinkhuis RF, Wijnholds J and Schinkel AH (1999) The mouse Bcrp1/Mxr/Abcp gene: amplification and overexpression in cell lines selected for resistance to topotecan, mitoxantrone, or doxorubicin. *Cancer Res* **59:**4237-4241.

Bardsley-Elliot A and Noble S (1999) Oseltamivir. *Drugs* **58:**851-860; discussion 861-852.

Breedveld P, Pluim D, Cipriani G, Wielinga P, van Tellingen O, Schinkel AH and Schellens JH (2005) The effect of Bcrp1 (Abcg2) on the in vivo pharmacokinetics and brain penetration of imatinib mesylate (Gleevec): implications for the use of breast cancer resistance protein and P-glycoprotein inhibitors to enable the brain penetration of imatinib in patients. *Cancer Res* **65:**2577-2582.

Brunner M, Langer O, Sunder-Plassmann R, Dobrozemsky G, Muller U, Wadsak W, Krcal A, Karch R, Mannhalter C, Dudczak R, Kletter K, Steiner I, Baumgartner C and Muller M (2005) Influence of functional haplotypes in the drug transporter gene ABCB1 on central nervous system drug distribution in humans. *Clin Pharmacol Ther* **78:**182-190.

Chowbay B, Cumaraswamy S, Cheung YB, Zhou Q and Lee EJ (2003) Genetic polymorphisms in MDR1 and CYP3A4 genes in Asians and the influence of MDR1 haplotypes on cyclosporin disposition in heart transplant recipients. *Pharmacogenetics* **13:**89-95.

Enokizono J, Kusuhara H and Sugiyama Y (2007) Role of Breast Cancer Resistance Protein (Bcrp/Abcg2) in the Disposition of Phytoestrogens : the Importance of Bcrp in the Efflux Transport in the Blood-Brain and -Testis Barriers. *Mol Pharmacol*.

Evers R, Kool M, Smith AJ, van Deemter L, de Haas M and Borst P (2000) Inhibitory effect of the reversal agents V-104, GF120918 and Pluronic L61 on MDR1 Pgp-, MRP1- and MRP2-mediated transport. *Br J Cancer* **83:**366-374.

Fromm MF (2002) The influence of MDR1 polymorphisms on P-glycoprotein expression and function in humans. *Adv Drug Deliv Rev* **54:**1295-1310.

Fuyuno I (2007) Tamiflu side effects come under scrutiny. *Nature* **446:**358-359.

Goralski KB, Acott PD, Fraser AD, Worth D and Sinal CJ (2006) Brain cyclosporin A levels are determined by ontogenic regulation of mdr1a expression. *Drug Metab Dispos* **34:**288-295.

Hasegawa T, Sugeno N, Takeda A, Matsuzaki-Kobayashi M, Kikuchi A, Furukawa K, Miyagi T and Itoyama Y (2007) Role of Neu4L sialidase and its substrate ganglioside GD3 in neuronal apoptosis induced by catechol metabolites. *FEBS Lett* **581:**406-412.

He G, Massarella J and Ward P (1999) Clinical pharmacokinetics of the prodrug oseltamivir and its active metabolite Ro 64-0802. *Clin Pharmacokinet* **37:**471-484.

Hill G, Cihlar T, Oo C, Ho ES, Prior K, Wiltshire H, Barrett J, Liu B and Ward P (2002) The anti-influenza drug oseltamivir exhibits low potential to induce pharmacokinetic drug interactions via renal secretion-correlation of in vivo and in vitro studies. *Drug Metab*

Dispos **30:**13-19.

Izumi T, Hosiyama K, Enomoto S, Sasahara K and Sugiyama Y (1997) Pharmacokinetics of troglitazone, an antidiabetic agent: prediction of in vivo stereoselective sulfation and glucuronidation from in vitro data. *J Pharmacol Exp Ther* **280:**1392-1400.

Izumi Y, Tokuda K, O'Dell K A, Zorumski CF and Narahashi T (2007) Neuroexcitatory actions of Tamiflu and its carboxylate metabolite. *Neurosci Lett* **426:**54-58.

Kikuchi R, Kusuhara H, Abe T, Endou H and Sugiyama Y (2004) Involvement of multiple transporters in the efflux of 3-hydroxy-3-methylglutaryl-CoA reductase inhibitors across the blood-brain barrier. *J Pharmacol Exp Ther* **311:**1147-1153.

Kikuchi R, Kusuhara H, Sugiyama D and Sugiyama Y (2003) Contribution of organic anion transporter 3 (Slc22a8) to the elimination of p-aminohippuric acid and benzylpenicillin across the blood-brain barrier. *J Pharmacol Exp Ther* **306:**51-58.

Kim RB (2002) MDR1 single nucleotide polymorphisms: multiplicity of haplotypes and functional consequences. *Pharmacogenetics* **12:**425-427.

Kimchi-Sarfaty C, Oh JM, Kim IW, Sauna ZE, Calcagno AM, Ambudkar SV and Gottesman MM (2007) A "silent" polymorphism in the MDR1 gene changes substrate specificity. *Science* **315:**525-528.

Kusuhara H and Sugiyama Y (2001) Efflux transport systems for drugs at the blood-brain barrier and blood-cerebrospinal fluid barrier (Part 1). *Drug Discov Today* **6:**150-156.

Lindegardh N, Davies GR, Tran TH, Farrar J, Singhasivanon P, Day NP and White NJ (2006) Rapid degradation of oseltamivir phosphate in clinical samples by plasma esterases. *Antimicrob Agents Chemother* **50:**3197-3199.

Maines LW, Antonetti DA, Wolpert EB and Smith CD (2005) Evaluation of the role of P-glycoprotein in the uptake of paroxetine, clozapine, phenytoin and carbamazapine by bovine retinal endothelial cells. *Neuropharmacology* **49:**610-617.

Matsuoka Y, Okazaki M, Kitamura Y and Taniguchi T (1999) Developmental expression of P-glycoprotein (multidrug resistance gene product) in the rat brain. *J Neurobiol* **39:**383-392.

Rousselle CH, Lefauconnier JM and Allen DD (1998) Evaluation of anesthetic effects on parameters for the in situ rat brain perfusion technique. *Neurosci Lett* **257:**139-142.

Sadeque AJ, Wandel C, He H, Shah S and Wood AJ (2000) Increased drug delivery to the brain by P-glycoprotein inhibition. *Clin Pharmacol Ther* **68:**231-237.

Sasongko L, Link JM, Muzi M, Mankoff DA, Yang X, Collier AC, Shoner SC and Unadkat JD (2005) Imaging P-glycoprotein transport activity at the human blood-brain barrier with positron emission tomography. *Clin Pharmacol Ther* **77:**503-514.

Satoh T, Taylor P, Bosron WF, Sanghani SP, Hosokawa M and La Du BN (2002) Current progress on esterases: from molecular structure to function. *Drug Metab Dispos* **30:**488-493.

Schinkel AH, Smit JJ, van Tellingen O, Beijnen JH, Wagenaar E, van Deemter L, Mol CA, van der Valk MA, Robanus-Maandag EC, te Riele HP and et al. (1994) Disruption of the mouse mdr1a P-glycoprotein gene leads to a deficiency in the blood-brain barrier and to increased sensitivity to drugs. *Cell* **77:**491-502.

Schinkel AH, Wagenaar E, van Deemter L, Mol CA and Borst P (1995) Absence of the mdr1a P-Glycoprotein in mice affects tissue distribution and pharmacokinetics of dexamethasone, digoxin, and cyclosporin A. *J Clin Invest* **96:**1698-1705.

Shi D, Yang J, Yang D, LeCluyse EL, Black C, You L, Akhlaghi F and Yan B (2006) Anti-influenza prodrug oseltamivir is activated by carboxylesterase human carboxylesterase 1, and the activation is inhibited by antiplatelet agent clopidogrel. *J Pharmacol Exp Ther* **319:**1477-1484.

Takano A, Kusuhara H, Suhara T, Ieiri I, Morimoto T, Lee YJ, Maeda J, Ikoma Y, Ito H, Suzuki K and Sugiyama Y (2006) Evaluation of in vivo P-glycoprotein function at the blood-brain barrier among MDR1 gene polymorphisms by using 11C-verapamil. *J Nucl Med* **47:**1427-1433.

Takasato Y, Rapoport SI and Smith QR (1984) An in situ brain perfusion technique to study cerebrovascular transport in the rat. *Am J Physiol* **247:**H484-493.

Tamai I and Tsuji A (2000) Transporter-mediated permeation of drugs across the blood-brain barrier. *J Pharm Sci* **89:**1371-1388.

Wiltshire H, Wiltshire B, Citron A, Clarke T, Serpe C, Gray D and Herron W (2000) Development of a high-performance liquid chromatographic-mass spectrometric assay for the specific and sensitive quantification of Ro 64-0802, an anti-influenza drug, and its pro-drug, oseltamivir, in human and animal plasma and urine. *J Chromatogr B Biomed Sci Appl* **745:**373-388.

Yamaguchi K, Hata K, Koseki K, Shiozaki K, Akita H, Wada T, Moriya S and Miyagi T (2005) Evidence for mitochondrial localization of a novel human sialidase (NEU4). *Biochem J* **390:**85-93.

Yamatsugu K, Kamijo S, Suto Y, Kanai M and Shibasaki M (2007) A concise synthesis of Tamiflu: third generation route via the Diels-Alder reaction and the Curtius rearrangement. *Tetrahedron Lett* **48:**1403-1406.

Footnotes

This study was supported by Grant-in-Aid for Scientific Research (A) from Japan Society for the Promotion of Science (JSPS) (KAKENHI 17209005).

Figure legends

Fig. 1. Chemical structures of oseltamivir (A) and Ro 64-0802 (B).

Fig. 2. Plasma concentration time profile (A) and brain-to-plasma concentration ratio ($K_{p, brain}$) (B) of oseltamivir and Ro 64-0802 following constant intravenous infusion of oseltamivir with and without GF120918 in FVB mice.

Mice received a constant intravenous infusion of oseltamivir at a dose of 8 μmol/hr/kg. GF120918 (10 mg/kg) was injected intravenously to mice 15 min before the intravenous infusion of oseltamivir. The plasma concentrations of oseltamivir and Ro 64-0802 were determined at designated time in control and GF120918-treated group (open and closed circles, respectively). The brain concentrations were determined at 120 min. Each point represents the mean ± S.E. (n = 3). Asterisks represent statistically significant differences between control and GF120918-pretreated mice; *, $P < 0.05$.

Fig. 3. Plasma concentration time profile (A) and brain-to-plasma concentration ratio ($K_{p, brain}$) (B) of oseltamivir and Ro 64-0802 following constant intravenous infusion of oseltamivir in Mdr1a/1b P-gp knockout, Bcrp knockout, and wild-type mice.

Mice received a constant intravenous infusion of oseltamivir at a rate of 8 μmol/hr/kg. The plasma concentrations of oseltamivir and Ro 64-0802 were determined at designated time in wild-type, Mdr1a/1b P-gp, and Bcrp knockout mice. The data for wild-type mice are shown by open circles, those for Mdr1a/1b P-gp knockout mice by closed squares, and those for Bcrp knockout mice by closed triangles. The brain concentrations were determined at 120 min. Each point represents the mean ± S.E. (n = 4-9). Asterisks represent statistically significant differences between wild-type and knockout mice; **, $P < 0.01$.

Fig. 4. Plasma concentration time profile (A), brain concentration (B), and brain-to-plasma concentration ratio ($K_{p, brain}$) (C) of oseltamivir and Ro 64-0802 following constant intravenous

infusion of oseltamivir in P3-P42 rats.

Rats received a constant intravenous infusion of oseltamivir at a rate of 8 μmol/hr/kg. The plasma concentrations of oseltamivir and Ro 64-0802 were determined at designated time in P3 (○), P6 (●), P11 (□), P21 (■) and P42 (◇) rats. The brain concentrations were determined at 60 min. Each point represents the mean ± S.E. (n = 4-6). Asterisks represent statistically significant differences toward P42 rats; **, $P < 0.01$.

Fig. 5. The mRNA expression of Mdr1a in the cerebral cortex from P3-P42 rats.

Total RNA was isolated from the cerebral cortex pooled from 1-4 rats, and then subjected to reverse transcription. The expression of mdr1a and gapdh mRNA in the cerebral cortex of P3-P42 rats was determined using real-time quantitative PCR. Each bar represents the mean ± S.E. of the ratio of the mRNA expression of mdr1a and gapdh. The quantification was repeated three times using three cDNAs independently prepared from 1-4 rats. Asterisks represent statistically significant differences toward P42 rats; **, $P < 0.01$.

Fig. 6. Ontogenetic expression of P-gp protein in the crude membrane fractions of cerebral cortex from P3-42 rats.

(A) Crude membrane fractions were prepared from the cerebral cortex from P3-42 rats. Each sample (50 μg protein/lane) was subjected to SDS-PAGE (8.5% separating gel). P-gp and actin proteins were detected by monoclonal anti-P-gp C219 antibody and monoclonal anti-actin antibody, respectively. A typical immunoblot is shown in panel (A). (B) The intensities of the bands of P-gp and actin were quantified by densitometric analysis. For P-gp, the intensity of the upper band was used for the calculation. The bar represents the ratio of the band densities of P-gp and actin relative to that in P42 rats. Each bar represents the mean ± S.E. of three determinations using three crude membrane fractions of the cerebral cortex prepared independently from 1-4 rats. Asterisks represent statistically significant differences toward P42 rats; *, $P < 0.05$.

Fig. 7. The stability of oseltamivir (A) and the formation of Ro 64-0802 (B) in plasma and liver S9 from newborn and adult rats.

Oseltamivir (1.5 μM) was incubated with rat plasma (circles) and liver S9 (squares) specimens (5 mg protein/mL) for various time periods. The data for adult (P42) rats are shown by open symbols, and for newborn (P11) rats by closed symbols. Data represent means ± S.E. of three determinations using three plasma and liver S9 specimens prepared independently from three rats.

Fig. 8. Cellular accumulation of oseltamivir in mouse Mdr1a-expressed LLC-PK1 cells (A) and human MDR1-expressed MDCKII cells (B).

The uptake of oseltamivir (2.5 μM) by mMdr1a-LLC-PK1 (A) and hMDR1-MDCKII (B) cells was examined in the presence or absence of PSC833 (5 μM) at 37 °C. Each point represents the mean ± S.E. (n = 4). Statistical significance was calculated by one-way ANOVA followed by Tukey's multiple comparison test.

DMD Fast Forward. Published on November 26, 2007 as DOI: 10.1124/dmd.107.018556
This article has not been copyedited and formatted. The final version may differ from this version.

Table 1. Ro 64-0802 formation rate from oseltamivir in plasma and liver S9 from newborn and adult rats.

Oseltamivir (1.5 μM) was incubated with rat plasma for 5 min and rat liver S9 fraction for 60 min at 37°C.

[a]Data represent means ± S.E. of three determinations using three plasma and liver S9 prepared independently from three rats.

[b]Obtained by multiplying the value (pmol/min/mg protein) by 50.0 and 96.1 for plasma and liver S9, respectively.

[C]Obtained by multiplying the value (pmol/min/mL plasma or g liver) by 38.5 and 40.0 for plasma and liver S9, respectively.

* $P < 0.05$ statistical differences in Ro 64-0802 formation rate (nmol/min/kg) in plasma between newborn and adult rats.

# $P < 0.05$ statistical differences in Ro 64-0802 formation rate (nmol/min/kg) in liver S9 between newborn and adult rats.

Source		Ro 64-0802 formation rate[a]		
		(pmol/min/mg protein)	(pmol/min/ml or g liver)	(nmol/min/kg BW)
plasma	P11	1.75 ± 0.32	87.7 ± 15.9	3.38 ± 0.61
	P42	10.6 ± 2.6	529 ± 129	20.4 ± 5.0*
liver S9	P11	0.11 ± 0.00	10.6 ± 0.3	0.42 ± 0.01
	P42	0.31 ± 0.05	29.7 ± 4.5	1.19 ± 0.18#

DMD Fast Forward. Published on November 26, 2007 as DOI: 10.1124/dmd.107.018556
This article has not been copyedited and formatted. The final version may differ from this version.

Fig. 1

(A) Oseltamivir

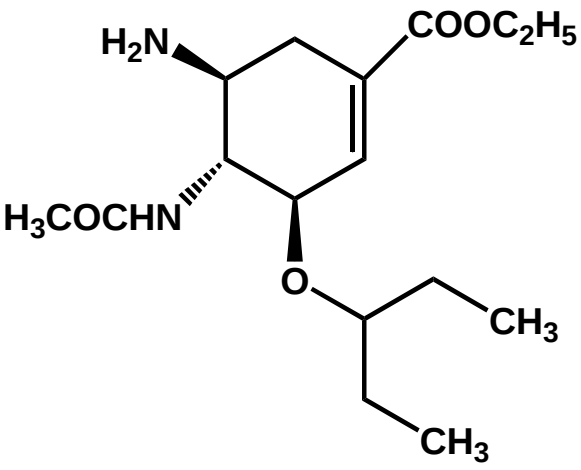

(B) Ro 64-0802

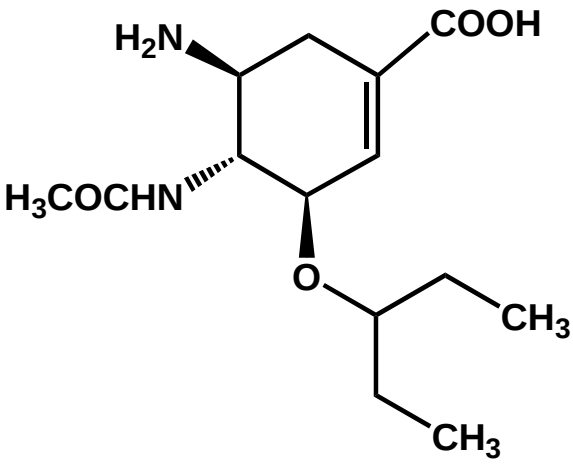

DMD Fast Forward. Published on November 26, 2007 as DOI: 10.1124/dmd.107.018556
This article has not been copyedited and formatted. The final version may differ from this version.

Fig. 2

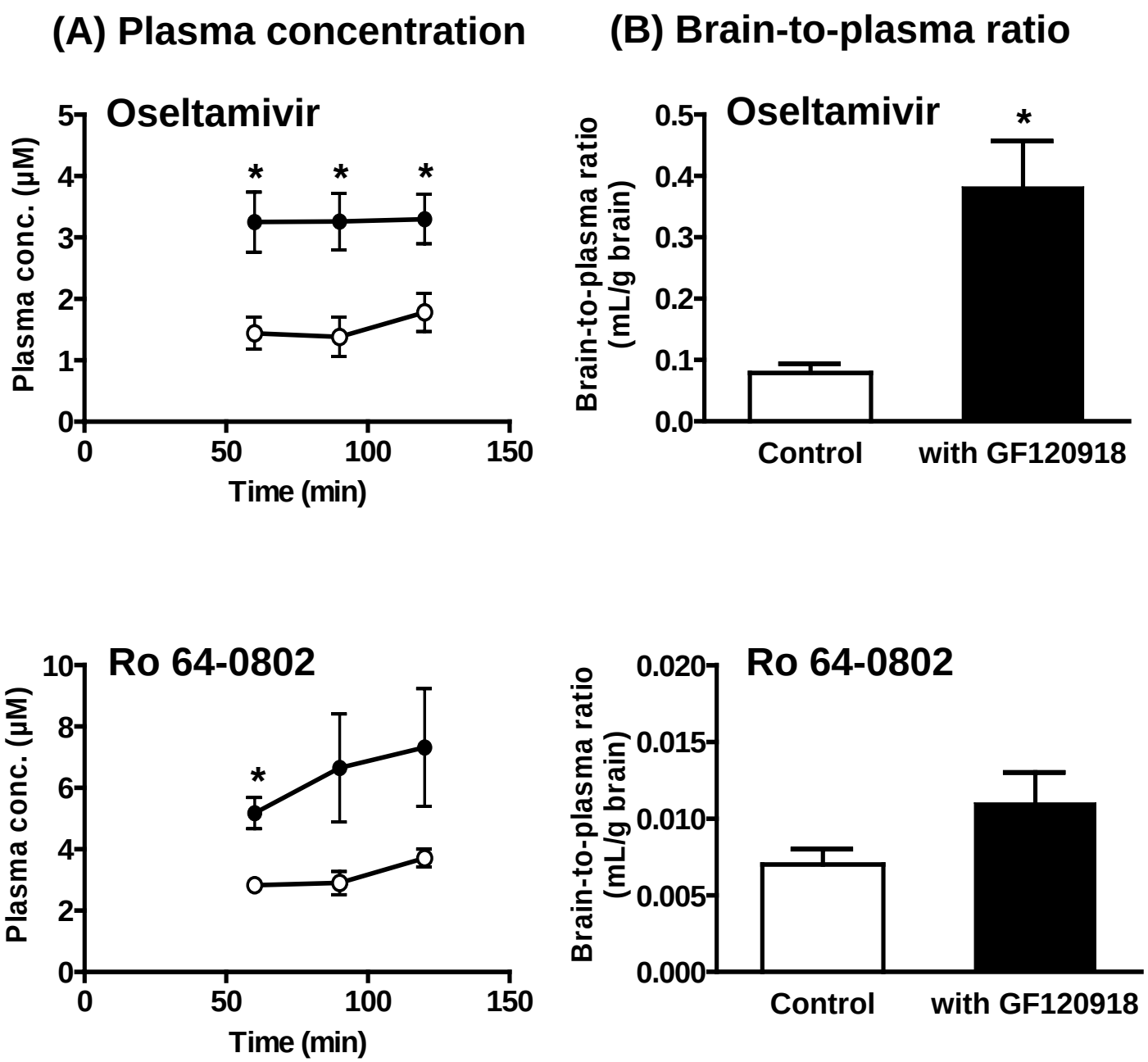

DMD Fast Forward. Published on November 26, 2007 as DOI: 10.1124/dmd.107.018556
This article has not been copyedited and formatted. The final version may differ from this version.

Fig. 3

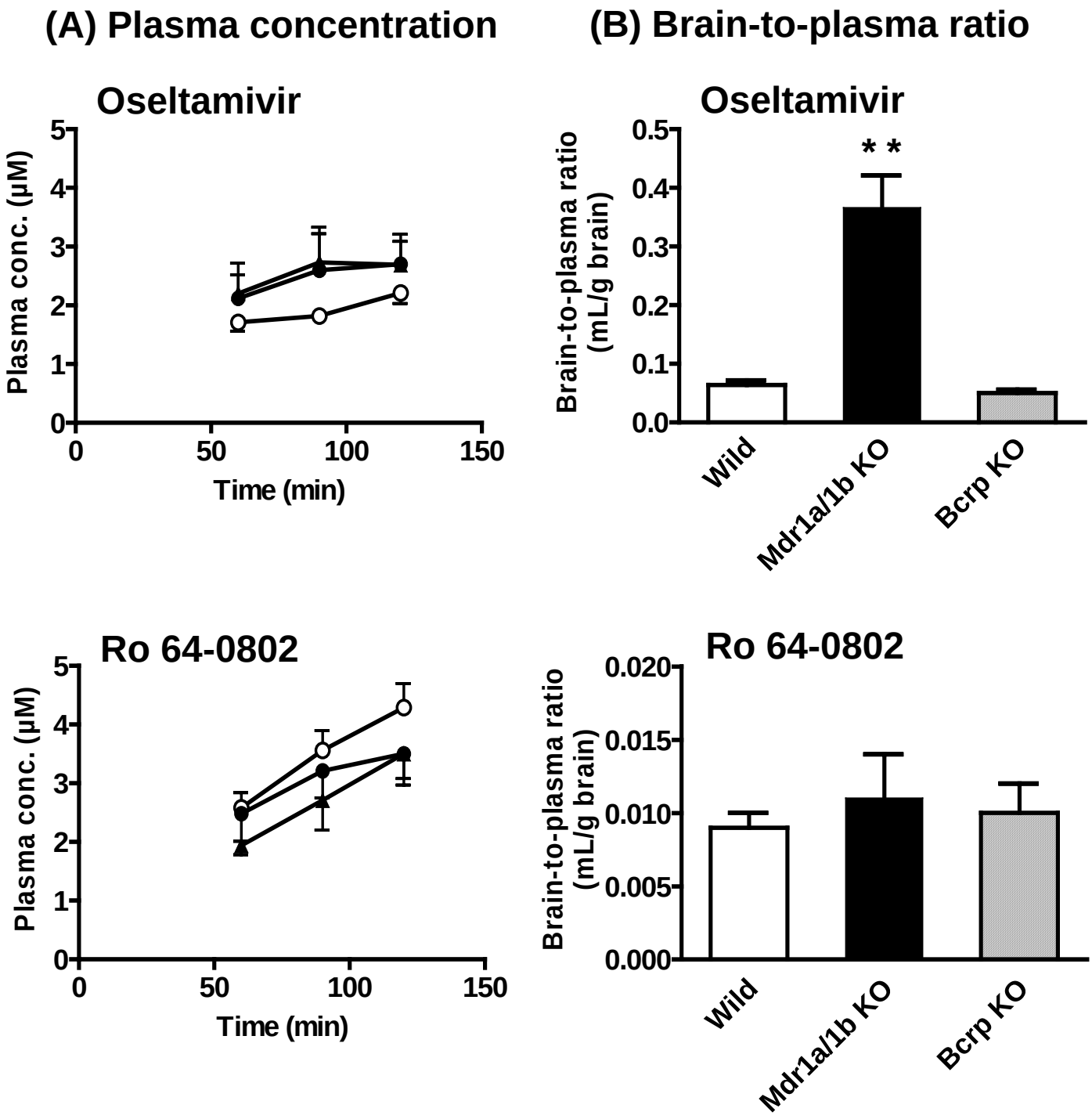

DMD Fast Forward. Published on November 26, 2007 as DOI: 10.1124/dmd.107.018556
This article has not been copyedited and formatted. The final version may differ from this version.

Fig. 4

(A) Plasma concentration

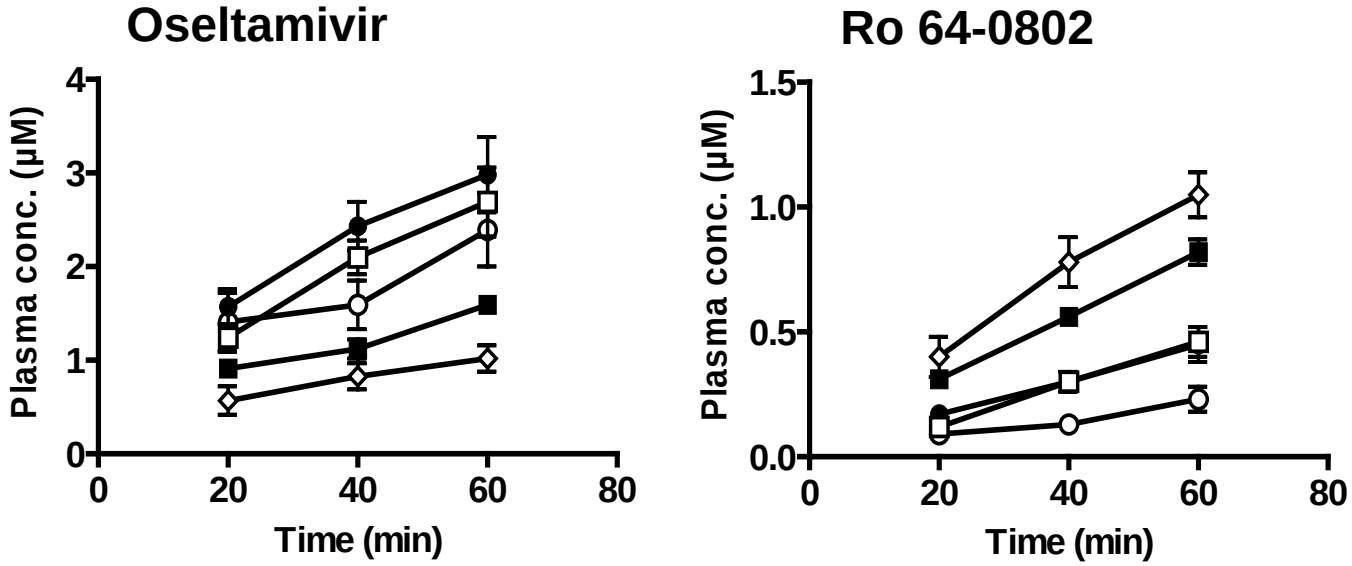

(B) Brain concentration

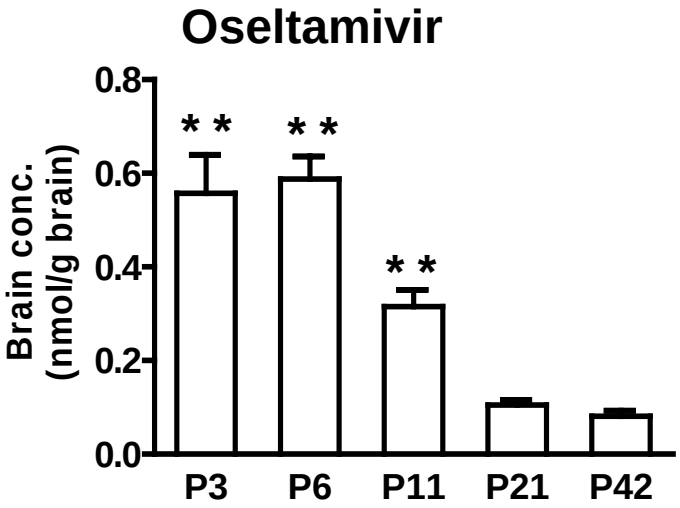

(C) Brain-to-plasma ratio

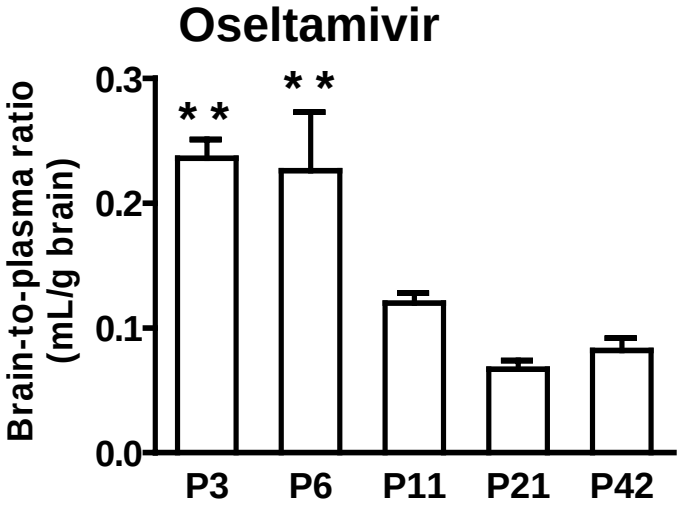

DMD Fast Forward. Published on November 26, 2007 as DOI: 10.1124/dmd.107.018556
This article has not been copyedited and formatted. The final version may differ from this version.

Fig. 5

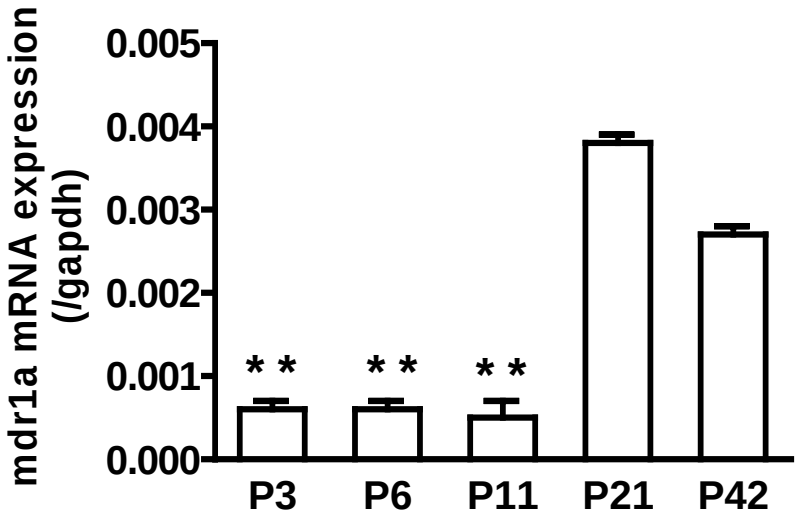

DMD Fast Forward. Published on November 26, 2007 as DOI: 10.1124/dmd.107.018556
This article has not been copyedited and formatted. The final version may differ from this version.

Fig. 6

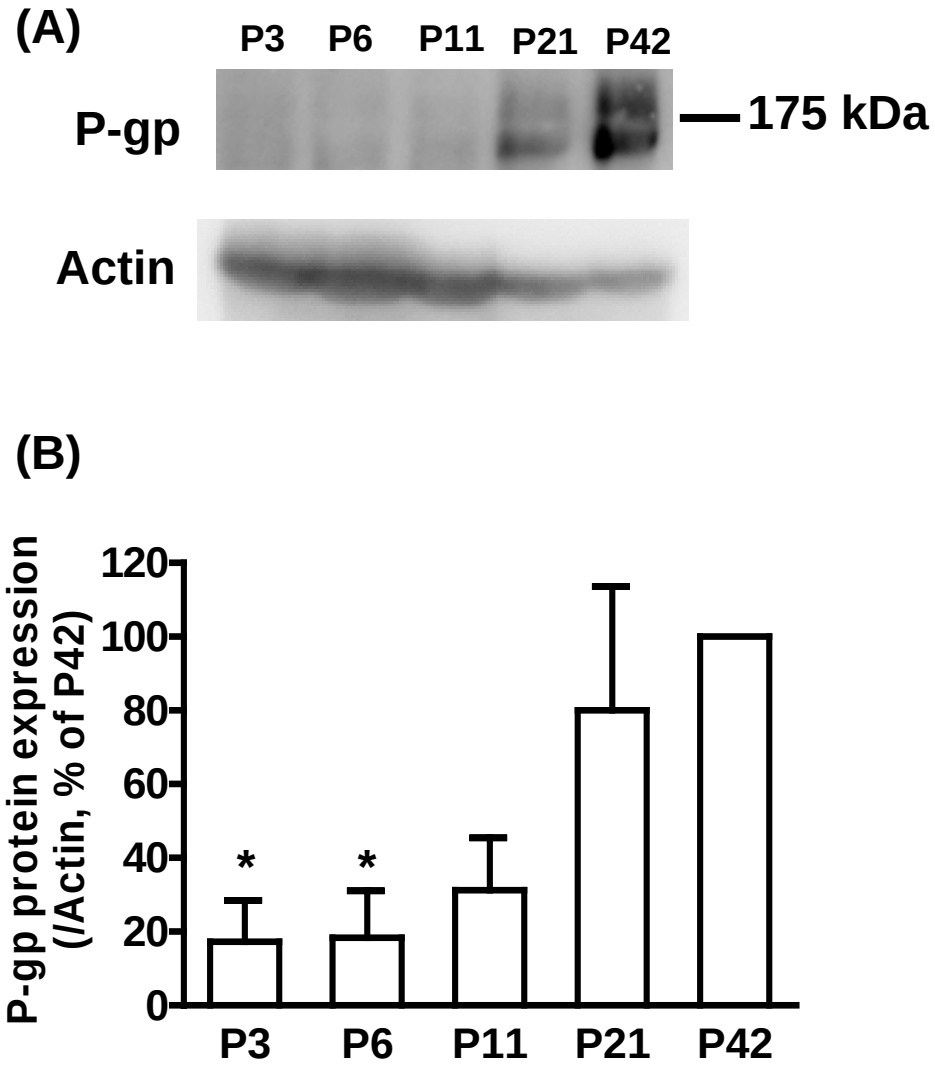

DMD Fast Forward. Published on November 26, 2007 as DOI: 10.1124/dmd.107.018556
This article has not been copyedited and formatted. The final version may differ from this version.

Fig. 7

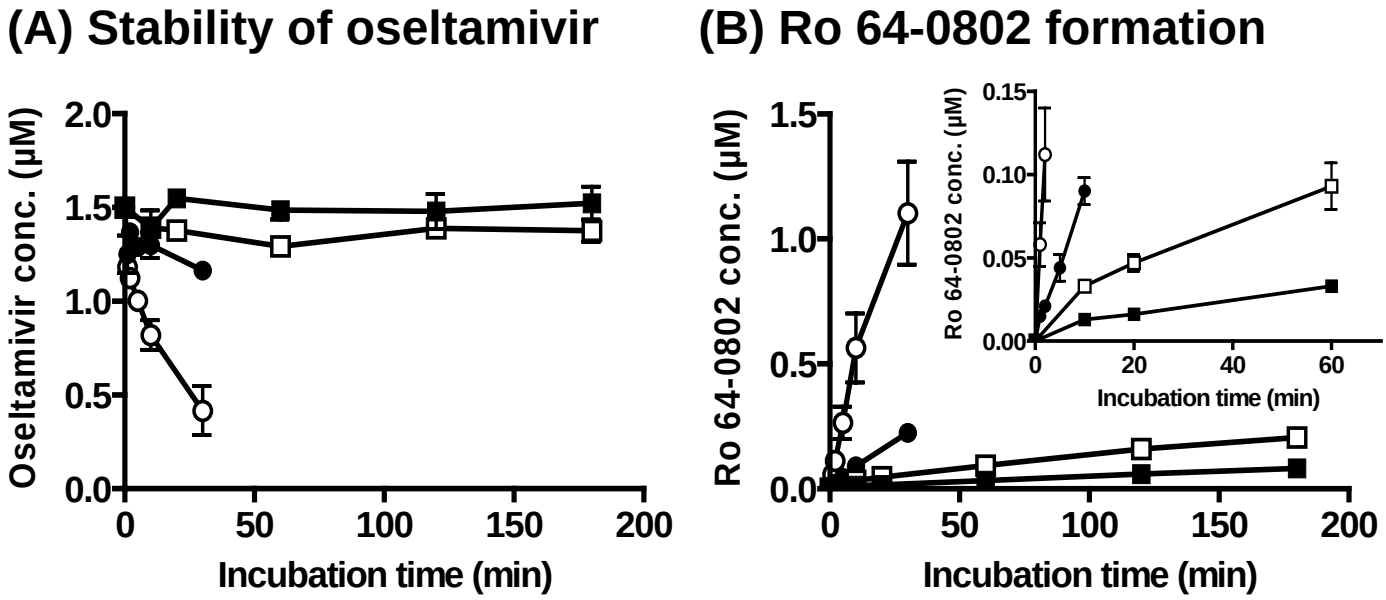

DMD Fast Forward. Published on November 26, 2007 as DOI: 10.1124/dmd.107.018556
This article has not been copyedited and formatted. The final version may differ from this version.

Fig. 8